Bottom-hinged Flap-type Wave Energy Converter with Efficient Mechanical Motion Rectifier

Jia Mi[#1], Lin Xu[#2], Beibei Liu[#3], Liang Sun[#4], Lei Zuo[*5]

[#]*Wuhan University of Technology, Wuhan, Hubei 430070, China, {[1]mj, [2]xulin508, [3]liubeibei, [4]liang.sun}@whut.edu.cn*

[*]*Virginia Tech, Blacksburg, VA 24061, USA, [5]leizuo@vt.edu*

Abstract— **Ocean wave energy is a renewable source that could reduce environmental impacts significantly than the traditional fossil energy. Many different ocean wave energy converters(OWECs), of various categories, have been proposed and prototyped, and power takeoff (PTO) system has been widely recognized as the most significant element for OWECs. Mechanical motion rectifier (MMR) has been used as a PTO system to harvest vibration energy for different applications and can achieve high energy conversion efficiency. This paper proposed a novel bottom-hinged flap-type energy converter with MMR to convert the bidirectional oscillation of the wave-surge flap to the unidirectional rotation of the generator. The working principle and dynamic modelling have been described in details, and the performance of MMR-based PTO has been verified by equivalent electric model. A small scale prototype has been tested in wave flume and the results show it can obtain 0.54W average power and 3.04W peak power with the excitation of 0.09m/2s.**

Keywords— **Ocean Wave, Mechanical Motion Rectifier, Power takeoff, Wave Energy, Energy Harvesting**

I. INTRODUCTION

Following with the prosperity from the development of modern industry, environmental contamination, natural resource damage and energy shortage have drawn public attention all over the world. What's more, the "food -energy - water" (FEW) nexus is central to sustainable development [1], The production as well as transportation of food and water cannot be done without energy, and energy is the bond between water and food, such as energy powered desalination to convert sea water into freshwater. What's more, the demand for all these three is increasing, driven by a rising global population, rapid urbanization, changing diets and economic growth. To solve this dilemma, people all over the world are searching for alternative clean energy, such as solar energy, nuclear power and biomass fuel.

Since vibration exists everywhere, from beating of the heart (mW) to oscillating motion of ocean waves (MW), it becomes a good alternative energy source and vibration energy harvesting has become a cutting-edge research in recent years. At the beginning, vibration energy harvesting mainly focused on resonance to power wireless sensors and low-power electronics. Large scale energy harvesting (>1W) has attracted more and more researchers due to its great potential, such as energy harvesting from human motion, vehicle and traffic, civil structures and ocean waves, and power takeoff (PTO) has been widely acknowledged as the most important element for vibration energy harvesting system [2]. As for ocean wave energy, there are various types of ocean wave energy converters (OWECs), with pros and cons for different marine regions[3]. In coastal region, offshore islands and atolls, oscillating wave surge converters (OWSCs) are typically utilized to exploit the enhanced horizontal fluid particle movement of waves. The simplest and the most stable type of device is a flap structure with its bottom edge hinged to the seabed [4].

Many researchers have investigated the bottom-hinged flap-type wave energy converters. In 2005, Aquamarine Power Ltd was formed to commercially develop "Power Oyster", and series of prototypes have been developed and tested [5]. In Finland, AW-Energy grows its supplier network and the first commercial WaveRoller was created alongside a rigorous technology qualification process validated by Lloyd's Register. The WaveRoller was manufactured, assembled, tested and certified in several locations around Europe during 2016-2017 [6]. In Australia, the bioWAVE was mounted on the seafloor, with a pivot axis near the bottom [7]. In America, Resolute Marine Energy has developed a technology that harnesses ocean wave energy to produce fresh water in areas where large-scale seawater desalination plants are too expensive and take too long time to build or where diesel-electric systems deliver limited quantities of high-cost water and add significant costs and environmental risks [8]. However, all of them use hydraulic cylinders to pressurize fluid and then convert the irregular hydraulic energy into continuous electricity. There are several disadvantages with the hydraulic transmission: 1) The transmission efficiency isn't very high for the viscous of fluid; 2) The harvested energy will be limited by the diameter of hydraulic cylinder; 3) The construction and maintenance will be difficult for the high pressure in the hydraulic system.

To solve all the aforementioned drawbacks, this paper proposes a novel bottom-hinged flap-type wave energy converter with efficient mechanical motion rectifier (MMR) [9]. The "shoaling" or "surge" motion of the waves near the shoreline with amplified horizontal movement of the water particles will drive the buoyant flap to rotate bidirectionally around the hinge fixed on the seabed. The MMR transforms the bidirectional rotations of the shaft into unidirectional rotation of the generator, with high efficiency, reliability, and less maintenance.

The rest of this paper is organized as follows. In Section 2, the design principle is introduced, and dynamic modelling of this MMR-based OWSC is developed. Experiment setup and

result for small scale prototype are introduced and discussed in Section 3.

II. DESIGN PRINCIPLE AND DYNAMIC MODELLING

A. Design principle

The overall design for the proposed bottom-hinged flap-type wave energy converter is shown in Figure 1. To capture "shoaling" or "surge" motion of the waves near the shoreline, the buoyant flap will be arranged heading to surge waves. There are two driving bevel gears on the flap shaft, between the shaft and driving bevel gears are one-way clutches. Because of these two one-way clutches, the bidirectional rotations of the shaft to the unidirectional rotation of the driven bevel gear and then drive the generator to generate electricity after rotation speed magnification by gearbox.

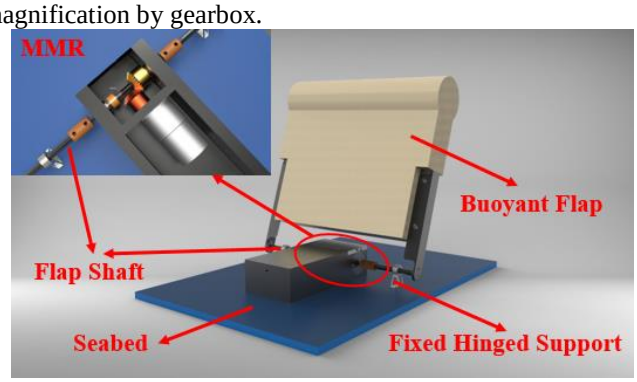

Fig. 1 Overall design

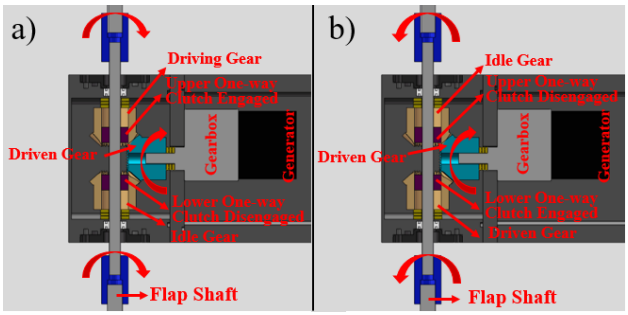

Fig. 2 Working principle of MMR

The working principle of MMR is shown in Figure 2. When the flap shaft rotates clockwise in Fig.2 (a), the upper one-way clutch engages but the lower one-way clutch disengages. Hence, the upper bevel gear becomes the driving gear but the lower bevel gear becomes the idle gear. In this condition, the driven gear rotates anticlockwise. When the flap shaft rotates anticlockwise in Fig.2 (b), the lower one-way clutch engages but the upper one-way clutch disengages. Hence, the lower bevel gear becomes the driving gear but the upper bevel gear becomes the idle gear. In this condition, the driven gear still rotates anticlockwise.

Because of these two one-way clutches, there are two phases in this system, engagement and disengagement. If the rotational speed of the flap shaft is larger than the rotational speed of driven gear, this system will be in engagement phase and the torque from buoyant flap will transmit to the PTO. If the rotational speed of the flap shaft is smaller than the rotational speed of driven gear, this system will be in disengagement phase and the torque from buoyant cannot transmit to PTO.

B. Dynamic model of the MMR-based PTO system

In rotational electromagnetic (EM) based energy harvesting system, the torque from PTO is made up of inertia torque $T_{inertia}$ and electromagnetic torque T_{EMF} [10]. As described in part A, there are two phases in this system.

In the engagement phase, the back electromotive torque is mainly induced by the back electromotive current of the generator and becomes an electrical damping in the system. The inertia force is mainly induced by the inertia of the rotational parts.

When the generator rotates, a back electromotive torque will be induced from generator, which can be expressed by

$$T_{EMF}=\frac{k_t k_e}{R_i+R_e} n_b n_g \frac{d\theta_g}{dt} \tag{1}$$

$$\frac{d\theta_g}{dt} = n_b n_g \frac{d\theta_s}{dt} \tag{2}$$

where n_g and n_b are the ratio of the gearbox and ratio of bevel gears, θ_g is the angular displacement the generator, θ_s is the angular displacement of the flap shaft, k_t (N*m/A) and k_e (V/(rad/s)) are, respectively, the voltage and torque constants of the generator, R_i and R_e are the internal and external resistance in the generator circuit.

As for another counteracting torque, it is induced by the inertia of the rotational mechanical components. Comparing with the generator inertia with gear ratio, the inertia from other components can be neglected, which can be expressed by

$$T_{inertia}=J_g n_b n_g \frac{d^2\theta_g}{dt^2} \tag{3}$$

$$\frac{d^2\theta_g}{dt^2} = n_b n_g \frac{d^2\theta_s}{dt^2} \tag{4}$$

where J_g is the inertia of the generator.

Hence, the total torque exerted from the MMR-based PTO system to flap shaft is

$$T_{MMR-PTO} = T_{EMF} + T_{inertia} \tag{5}$$

Plug Eq. (1)-(6) to Eq. (7), the total torque from PTO can be expressed as

$$T_{MMR-PTO} = I_e \frac{d^2\theta_s}{dt^2} + c_e \frac{d\theta_s}{dt} \tag{6}$$

where $I_e = J_g n_b^2 n_g^2$, $c_e = \frac{k_t k_e}{R_i+R_e} n_b^2 n_g^2$.

The first portion of the torque in Equation (8) is proportional to relative angular acceleration of the flap, therefore I_e can be seen as equivalent inertia of the MMR-based PTO system. The second portion of the torque is proportional to the relative angular velocity if the flap, and c_e is the equivalent damping of the MMR-based PTO system.

In the disengagement phase, three bevel gears and gearbox will rotate with the generator with the following equation:

$$J_g n_b^2 n_g^2 \frac{d^2\theta_b}{dt^2} + \frac{k_t k_e}{R_i+R_e} n_b^2 n_g^2 \frac{d\theta_b}{dt} = 0 \tag{7}$$

where θ_b is the angular displacement of the driving gear.

According to Equation (4), the rotation speed ω_r of the driving bevel gears will decrease exponentially after disengagement happens:

$$\frac{d\theta_b}{dt} = \left(\frac{d\theta_b}{dt}\right)_{t_0} e^{-\frac{t-t_0}{\tau}} \tag{8}$$

where $\left(\frac{d\theta_b}{dt}\right)_{t_0}$ is the rotational speed of the driving bevel gears when disengagement happens, τ is the time constant $\tau = I_e/c_e$.

When the rotational speed of the driving bevel gears decreases and equals to input rotational speed of the flap shaft, this system will be engaged again.

Hence, the torque from the PTO system can be expressed as

$$\begin{cases} T_{PTO} = I_e \frac{d^2\theta_s}{dt^2} + c_e \frac{d\theta_s}{dt} & Engagement \\ T_{PTO} = 0 & Disengagement \end{cases} \tag{9}$$

C. *Dynamic model of the oscillating surge wave energy converter with MMR*

The equation of motion for a floating body, about the center of gravity can be expressed as

$$I\frac{d^2\theta}{dt^2} = T_{ext} + T_{rad} + T_B + T_m + c_v\frac{d\theta}{dt} + T_{PTO} \tag{10}$$

where I is the inertia of the flap, T_{ext} is the wave excitation torque, T_{rad} is the wave radiation torque, T_B is the net buoyancy restoring torque, T_m is the torque due to mooring connection, c_v is the viscous damping.

As for the traditional PTO without MMR, it can be defined as NonMMR-PTO, the torque from NonMMR-PTO system can be written as

$$T_{Non-PTO} = I_e\frac{d^2\theta_s}{dt^2} + c_e\frac{d\theta_s}{dt} \tag{11}$$

Hence, the governing equation of the NonMMR-based PTO system can be expressed as:

$$(I + I_e)\frac{d^2\theta_s}{dt^2} = T_{ext} + T_{rad} + T_B + T_m + (c_v - c_e)\frac{d\theta_s}{dt} \tag{12}$$

As described in section Ⅱ-B, the MMR-based PTO system is a nonlinear system for the engagement and disengagement of the one-way clutches.

Based on Equation (11), the motion equation in the engaged phase can be expressed as

$$(I + I_e)\frac{d^2\theta_s}{dt^2} = T_{ext} + T_{rad} + T_B + T_m + (c_v - c_e)\frac{d\theta_s}{dt} \tag{13}$$

As for the disengaged phase, the equation of motion of this system becomes two decoupled equations:

$$\begin{cases} I\frac{d^2\theta_s}{dt^2} = T_{ext} + T_{rad} + T_B + T_m + c_v\frac{d\theta_s}{dt} \\ J_g n_b^2 n_g^2\frac{d^2\theta_b}{dt^2} + \frac{k_t k_e n_b^2 n_g^2}{R_i + R_e}\frac{d\theta_b}{dt} = 0 \end{cases} \tag{14}$$

D. *Simulation of the MMR-based PTO system*

As described in section B, there are engagement and disengagement in this proposed MMR-based PTO system, hence, the dynamics of this system is not linear. But it can be seen as a sectionalized linear system, which means that each phase is linear but for the overall process is nonlinear, and the threshold between these two phases are determined by the inertia of the generator and parameters of the generators' constants. For such a nonlinear system, it's very complicated to derive the closed-form solution. The MMR with two roller clutches can be compared to a full-wave voltage rectifier using a center-tapped transformer and two diodes [9,11], as shown in Figure 3. And the equivalent electric model can be realized in commercial software, like Simulink, as shown in Figure 4.

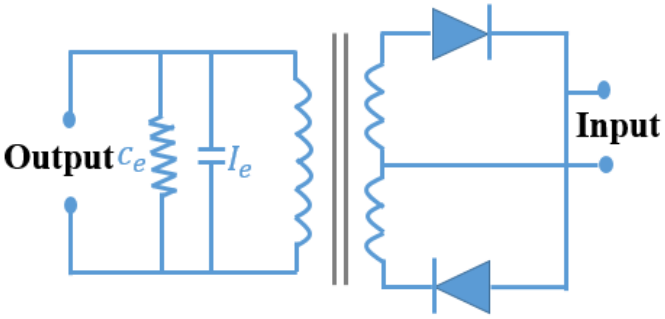

Fig. 3 Electrical analogue for MMR

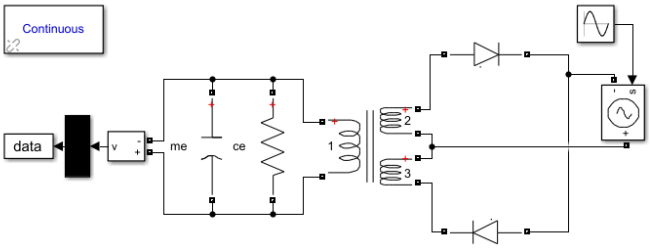

Fig.4 Equivalent electric model in Simulink

The performance of the equivalent electric model of the MMR-based PTO can be seen in Figure 5. The line in blue is the input speed, and the line in red shows the output speed, it shows that the input speed and output speed are the same in the engaged period, but when the disengagement happens, the output speed will decay in a certain ratio.

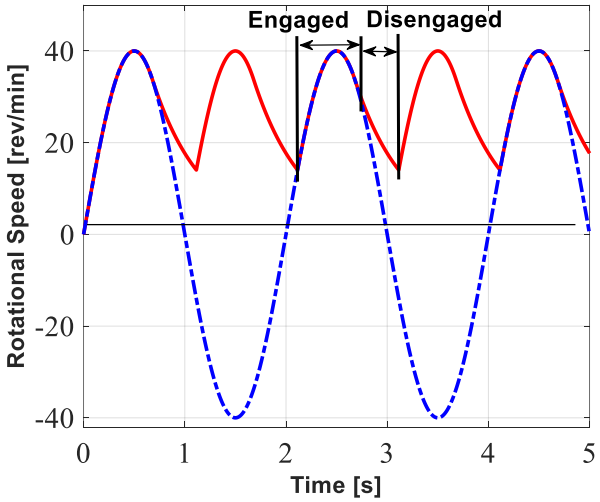

Fig.5 Performance of MMR

III. EXPERIMENT SETUP AND RESULTS DISSCUSSION

A. *Test condition*

To validate the performance of the proposed MMR-based OSWEC, a small-scale prototype is fabricated and tested in the wave flume of *Laboratory of Fluid* in Wuhan University of Technology (WUT). The schematic of the wave flume and layout of the devices is shown in Figure 6. The ranges of the wave height and wave period in this flume are 0-0.15m/ 0.5-3.5s.

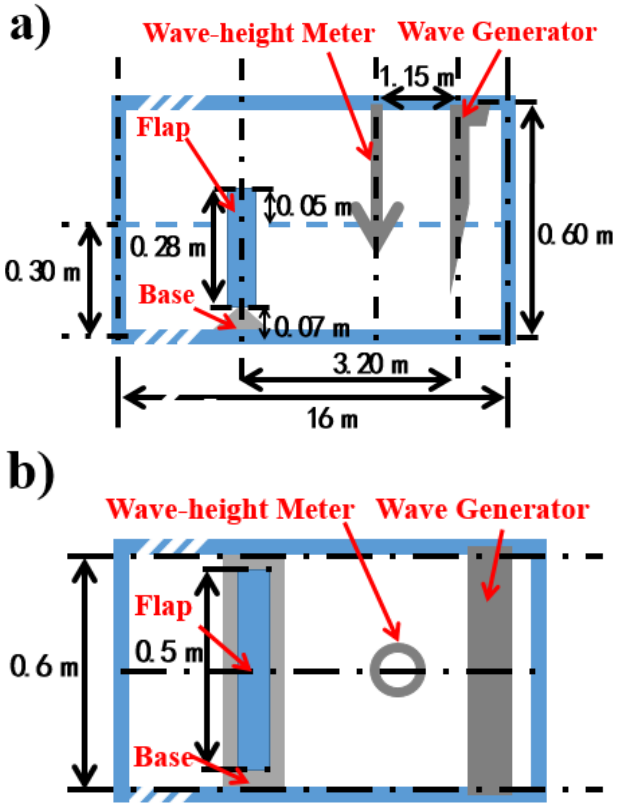

Fig.6 Schematic of the wave flume and layout of the devices. a) Side view b) Top view

As described in 2, external resistance will affect the equivalent electric damping of the MMR-based PTO, and then affect the harvestable electric energy. Hence, a suitable external resistance is important in the experiment. To adjust the external resistance and measure the test data, an electronic load is used and the test condition can be seen in Figure 7.

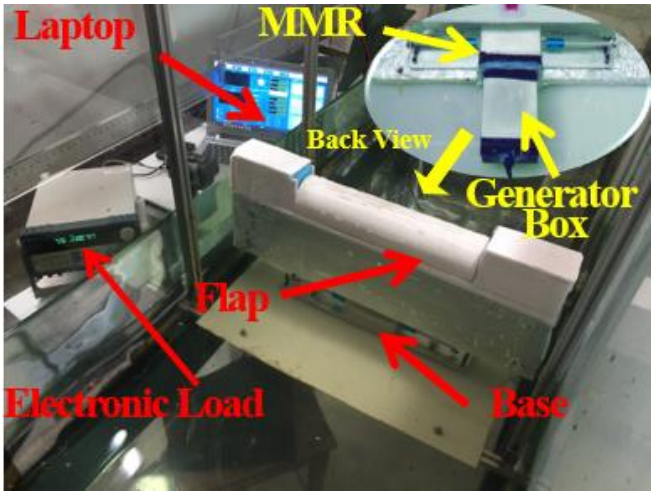

Fig. 7 Photograph of the prototype and measurement devices

During the test, the parameters to generate specific waves are inputted by host computer by its inner software. The amplitude and period of the wave generator can determine the generated wave-height and period, so the wave generator should be calibrated by the wave-height meter for each target wave, and the final parameters for each test are subjected to the parameters measured by the wave-height meters. It should be noted that, the distance between wave generator and wave-height meter as well as flap will affect the actual waves impacting on the flap. What's more, limited by the length of the flume, the reflection of the waves from the end of the flume and the flap itself will also affect the actual waves acting on the flap, we just choose the data during valid range to analyse, and test for each wave condition will be done twice to avoid accidental.

After the aforementioned calibration, the wave-height detected by the weight-height meter in a sample condition (50mm/3s) is shown in figure 8. From figure 8, we can see there are three periods in each test, the ramp period reprents the preparation period of the wave generator, the valid period reprents the waves form is valid as the setting in the host computer, the superimposed period reprents that some waves are reflected from the end of the flume and the flap itself will also generate waves. Hence, we should only analyse the results during the valid period in each test. From the test outcome of wave-height meter, the waves form during the valid period is very close to the pre-set value in the host computer, an assumption is made that the actual waves form during the valid period is the pre-set value in the host computer in the following test.

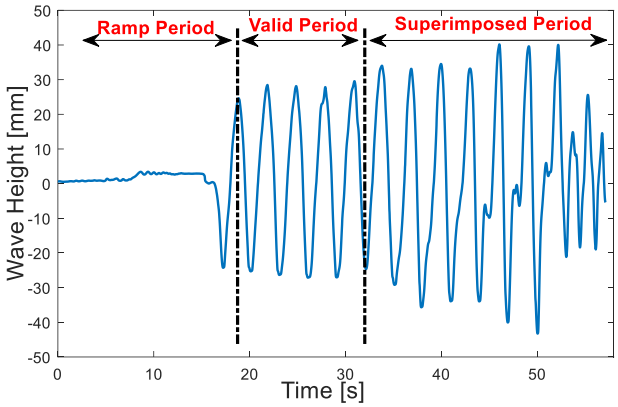

Fig.8 Wave-height meter data of a sample condition(50mm/3s)

B. Test results and discussion

The generator used in this system is a 20W graphite brushes motor (nominal voltage 24V/ gear ratio 1:236) produced by Maxon, and its internal resistance is 2.32 Ω. In order to find a suitable external resistance to achieve high efficiency, a series tests with several external resistances were done (wave-height 0.05m/period 2s), and the result is shown in figure 9.

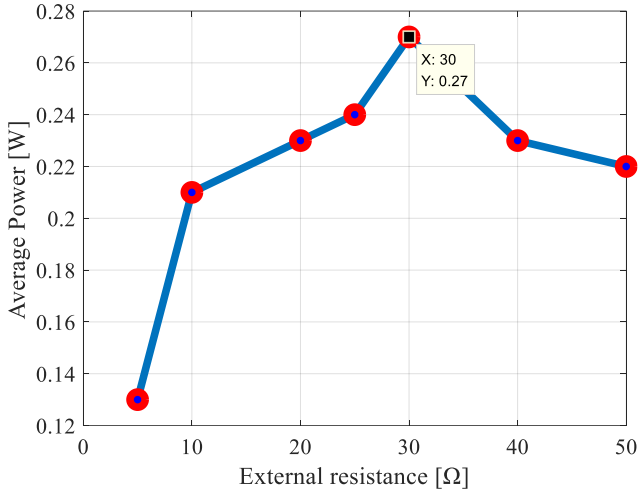

Fig.9 Average power at different external resistance (wave condition 0.05m/2s)

From results in figure 9, the best external resistance is 30 Ω. Hence, we set the external resistance as 30 Ω in all the following tests.

In order to verify the influence of wave-height and period to this system, a series of wave-height (0.05m/0.07m/0.09m) and wave-period (1s/1.5s/2s/2.5s/3s) were chosen, as shown in figure 10 and 11. It should be noted that the wave generator cannot generate the wave form at 0.09m/1s, hence, the results in figure 10 and 11 at this point are blank.

From the results in figure 10 and 11, the best wave period for this prototype is about 2s, and the average power and peak power at 0.09m/2s can reach 0.53W and 3.04W, respectively, which means that the natural frequency of the flap is about 2s, and it will resonate when the wave period is close to the natural frequency.

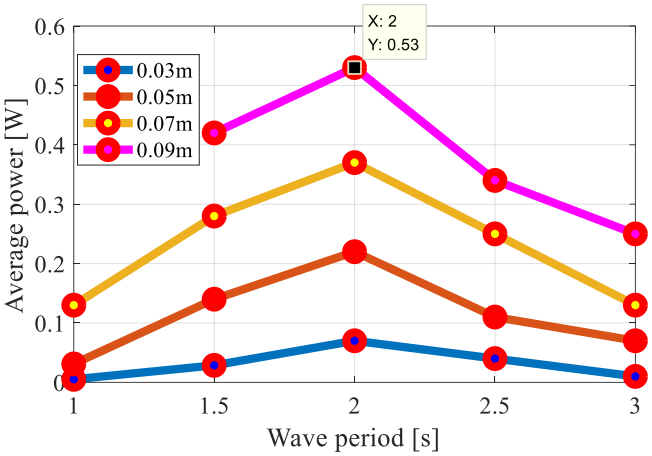

Fig. 10 Average power at several wave conditions

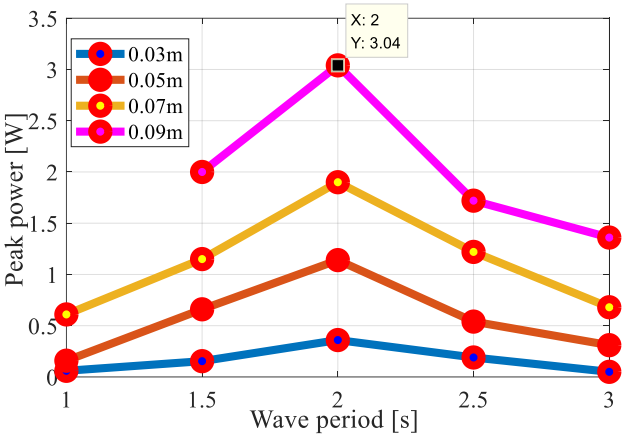

Fig. 11 Peak power at several wave conditions

The instant power with the excitation of 0.09m/2s is shown in figure 12, the engaged period and disengaged period are shown in this figure, which can verify the simulation in section 2. In addition, there are two peaks in each period, the higher one is in head waves and the lower on is in back waves. What's more, the peak power is about 3.04W, but the nominal power is 20W of the selected generator, which means the generator used in this system is not very suitable for the input speed cannot reach to the high efficiency range.

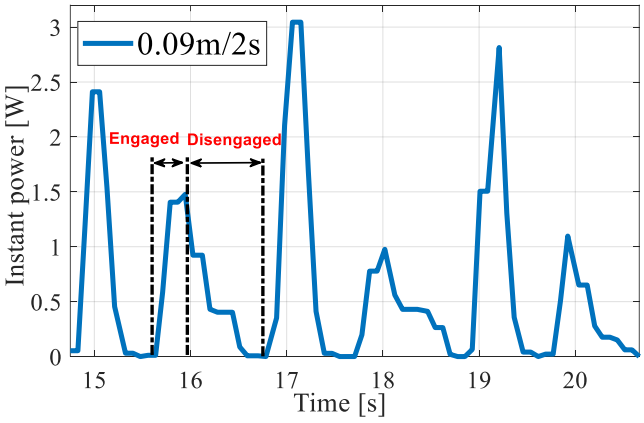

Fig.12 Instant power at 0.09m/2s

IV. CONCLUSIONS

In this paper, following progresses are reported.

1. A novel bottom-hinged flap-type wave energy converter with efficient mechanical motion rectifier has been proposed, and the design principle as well as dynamic modelling are introduced.
2. There are engaged and disengaged period in the proposed MMR-based PTO, and its performance has been simulated by equivalent electric model.
3. A small scale prototype has been tested in the wave flume, the results shows that the natural period of the flap is about 2s. This system can obtain 0.53W average power and 3.04W peak power with excitation 0.09m/2s. And the engagement and disengagement of the MMR-based PTO are shown in the test.

The hydrodynamics modelling will be reported in the final paper submission.

ACKNOWLEDGMENT

The authors gratefully acknowledge the financial supports from National College Students Innovation and Entrepreneurship Training program of China (Project #20171049707019) and the U.S. - Egypt Science and Technology Joint Fund (Project #1047). We would thank support from Shock-En Technology Studio. We thank Junyi Zou, Mohamed A.A Abdelkareem, Mingyi Liu for the modelling discussion, and Xiaosa Zhao and Xiaowei Zheng of for their help in the wave flume test.

REFERENCES

[1] L. Bizikova, D. Roy, D. Swanson, and M. Venema, Henry David, McCandless, "The Water-energy-food Security Nexus: Towards a Practical Planning and Decision-support Framework for Landscape Investment and Risk Management," *Int. Inst. Sustain. Dev.*, no. February, p. 28, 2013.

[2] L. Zuo and X. Tang, "Large-scale vibration energy harvesting," *J. Intell. Mater. Syst. Struct.*, vol. 24, no. 11, pp. 1405–1430, 2013.

[3] J. Xie and L. Zuo, "Dynamics and control of ocean wave energy converters," *Int. J. Dyn. Control*, vol. 1, no. 3, pp. 262–276, 2013.

[4] Whittaker, T., Folley, M., Causon, D. M., Ingram, D. M. & Mingham, C. G. 2005 An experimental and numerical study of oscillating wave surge converters. EPSRC report GR/S12326/01.

[5] Aquamarine Power Ltd. Oyster. See http://www.aquamarinepower.com.

[6] AW-Energy Oy. WaveRoller. See http://www.aw-energy.com.

[7] BioPower Systems Pty. Ltd.BioWAVE.See http://www.biopowersystems.com.

[8] Resolute Marine Energy. See http://www.resolutemarine.com/

[9] Z. Li, L. Zuo, J. Kuang, and G. Luhrs, "Energy-harvesting shock absorber with a mechanical motion rectifier," *Smart Mater. Struct.*, vol. 22, no. 2, 2013.

[10] S. Guo, Y. Liu, L. Xu, X. Guo, L. Zuo, Performance evaluation and parameter sensitivity of energy-harvesting shock absorbers on different vehicles. *Vehicle System Dynamics*, vol. 54, (7), pp. 918-942, 2016.

[11] P.C. Breedveld, 2008 Modeling and simulation of dynamic systems using bond graphs, *Control Systems, Robotics and Automation*, Edited by Heinz Unbehauen, Encyclopedia of Life Support Systems (EOLSS), Eolaa Publishers, Oxford, UK